field and that the relative complex permeability of the material be of unit magnitude. Limitations for practical sorting systems in terms of accuracy, stability, and object properties are to be determined. Also, a variety of other types of microwave resonators could be used for this purpose.

References

[1] H. E. Bussey, "Measurement of RF properties of materials—A survey," *Proc. IEEE*, vol. 55, pp. 1046–1053, 1967.

[2] Standard Test Methods D-2520-81, "Complex permittivity of solid electrical insulating materials at microwave frequencies and temperatures to 1650°C," Amer. Soc. for Testing and Materials, Philadelphia, PA.

[3] W. Rueggeberg, "Determination of complex permittivity of arbitrarily dimensioned dielectric modules at microwave frequencies," *IEEE Trans. Microwave Theory Tech.*, vol. MTT-19, pp. 517–521, June 1971.

[4] M. L. Lakshminarayana, L. D. Partain, and W. A. Cook, "Simple microwave technique for independent measurement of sample size and dielectric constant with results for a Gunn oscillator system," *IEEE Trans. Microwave Theory Tech.*, vol. MTT-27, pp. 661–665, July 1979.

[5] W. Hoppe, W. Meyer, and W. Schilz, "Density-independent moisture metering in fibrous materials using a double-cutoff Gunn oscillator," *IEEE Trans. Microwave Theory Tech.*, vol. MTT-28, pp.1449–1452, Dec. 1980.

[6] A. W. Kraszewski, T.-S. You, and S. O. Nelson, "Microwave resonator technique for moisture content determination in single soybean seeds," *IEEE Trans. Instrum. Meas.*, vol. 38, pp. 79–84, Feb. 1989.

[7] R. F. Harrington, *Time-Harmonic Electromagnetic Fields*. New York: McGraw-Hill, 1961, p. 321.

[8] R. A. Waldron, *The Theory of Waveguides and Cavities*. London: Maclaran and Sons, 1976, p. 75.

[9] H. Altschuler, in *Handbook of Microwave Measurements*, vol. 2, M. Sucher and J. Fox, Eds. Brooklyn, NY: Polytechnic Press, 1963, pp. 530–536.

[10] W. B. Westphal and A. Sils, *Dielectric Constant and Loss Data*, Tech. Rep. AFML-TR-72-39, Air Force Materials Laboratory, Air Force Systems Command, Wright-Patterson Air Force Base, Ohio, 1972, p. 161.

Efficient Computation of High-Frequency Two-Dimensional Effects in Multiconductor Printed Interconnects

Lawrence Carin

Abstract—**The spectral domain technique with a Galerkin moment method solution is used to study high-frequency, two-dimensional effects such as dispersion and leakage in multiconductor printed interconnects. A simple asymptotic procedure is used to significantly improve the convergence of oscillatory spectral integrals involving distant expansion and testing functions. Examples are given for leaky waves on two multiconductor printed transmission line geometries.**

Manuscript received September 25, 1990; revised June 11, 1991. This work was supported in part by the New York State Center for Advanced Telecommunications Technology.

The author is with the Electrical Engineering Department, Polytechnic University, Farmingdale, NY 11735.

IEEE Log Number 9103899.

I. Introduction

Multiconductor transmission lines have been the interest of numerous researchers for several decades. Recently, there has been much interest in multiconductor printed transmission lines used as interconnects in high-speed integrated circuits [1], [2]. In this paper, concentration will be placed on developing an asymptotic technique for the efficient numerical analysis of high-frequency, two-dimensional effects such as dispersion and leakage in printed interconnects.

The numerical analysis is formulatd in the spectral domain with a Galerkin moment method solution [1], [2]. Although this method is well known, special care must be taken when studying high-frequency effects such as dispersion and leakage. The reaction integrals which must be evaluated in the moment method solution are often highly oscillatory. This is especially true for the problem at hand: since a multiconductor system is considered, expansion and testing functions will often be relatively far apart in space. This coupled with the fact that leakage and dispersion usually are important at relatively high frequencies, leads to spectral integrals which are often highly oscillatory and hence CPU intensive.

Oscillatory integrals occur often in electromagnetic problems and therefore several asymptotic techniques have been developed for their evaluation. Much previous work has been directed at the investigation of three-dimensional layered problems and has led to analyses which, although general, are more complicated than what is needed in this two-dimensional study. In three-dimensional layered problems, each matrix component in a moment method solution consists of a double inverse Fourier transform (found using a plane wave spectral formulation) [3]. Only under very special conditions (see Appendix I of [4]), not possible for most practical testing and expansion functions, can this double integral be reduced to a one-dimensional Sommerfeld type integral. Hence, most previous asymptotic treatments of spectral integrals have dealt with the efficient computation of the Green's function [5], [6], which for a three (or two) dimensional layered problem can be written as a single semi-infinite integral of the Sommerfeld type [4]. In these approaches, after efficiently determining the space domain Green's function, one is still required to evaluate space domain integrals involving expansion and testing functions. The key difference between the asymptotic procedure developed here and those used previously for three-dimensional problems is that for distant expansion and testing functions, the entire matrix component is efficiently evaluated asymptotically in the spectral domain, without the need for subsequent space domain integration.

In Section II, the spectral domain technique is briefly reviewed and then, by considering the physical nature of modes on printed interconnects, an efficient asymptotic technique is developed for studying high-frequency effects in multiconductor printed interconnects. The asymptotic technique is then used to study leaky waves on two example structures, and the results are compared with data in the literature.

II. Analysis

A. Formulation

The spectral domain technique with a Galerkin moment method solution [1], [2] will be used to calculate the complex propagation constants for multiconductor printed transmission lines, such as that depicted in Fig. 1. This analysis results in a matrix equation with

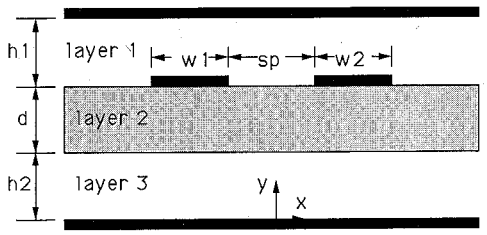

Fig. 1. Layered printed transmission geometry for which results are given in this paper. Layers 1 and 3 are air and layer 2 has dielectric constant ϵ_r.

components of the form

$$\int_C \tilde{J}^*_{tk}(k_x, y)\,\tilde{G}_{kl}(\gamma, k_x, y; y')\,\tilde{J}_{el}(k_x, y')\,e^{jk_x\Delta}\,dk_x \qquad (1)$$

where $\tilde{G}_{kl}(\gamma, k_x, y; y')$ is the spectral dyadic Green's function component for a k-directed electric field component located at y due to an l-directed surface current located at y', $\tilde{J}_{el}(k_x, y')$ is an l-directed expansion current in the spectral domain located at y', $\tilde{J}_{tk}(k_x, y)$ is a k-directed testing function in the spectral domain located at y, and Δ is the distance in x between the centers of the testing and expansion functions in the space domain. In (1), l and k can both be either x or z and the superscript * denotes complex conjugate. The spectral integral exists on the real axis unless poles are encountered and/or integration around branch cuts is required. In (1) it is assumed the modes have an $e^{-j\gamma z}$ longitudinal dependence ($\gamma = \beta - j\alpha$).

In printed transmission line applications, one usually operates in a regime in which all higher order modes are below cutoff and are therefore only of importance at discontinuities (which are not addressed here). This paper will therefore concentrate on the $N-1$ zero-cutoff-frequency modes in an N conductor system [1]. Since these modes are slow-waves, no radiation into space-waves will exist. Hence an open physical structure (no top and/or bottom conducting surfaces) can be accurately modeled by placing conducting covers far from the transmission lines where all evanescent fields have decayed sufficiently. Therefore, in the analysis to follow, only geometries with top and bottom conducting surfaces will be considered and leakage (if present) will be in the form of parallel plate modes. Since only shielded (on top and bottom) geometries are to be studied, there will be no branch cuts in the complex k_x plane.

It can be shown that each component of the dyadic spectral Green's function for planar strips in a layered dielectric medium can be written in the form

$$\tilde{G}_{kl}(\gamma, k_x, y; y') = \frac{f(\gamma, k_x, y; y')}{D_{\mathrm{TE}}(\gamma^2 + k_x^2)\,D_{\mathrm{TM}}(\gamma^2 + k_x^2)} \qquad (2)$$

where $D_{\mathrm{TE}}(\Gamma^2) = 0$ and $D_{\mathrm{TM}}(\Gamma^2) = 0$ are transcendental equations for TE and TM modes, respectively, in the layered dielectric medium under study (with no conducting strips). If there are top and bottom conducting plates (as in the case considered here), these modes correspond to parallel plate modes; otherwise, the modes correspond to surface waves. In either case, the propagation constant (imaginary if below cutoff) of the TE or TM mode is Γ.

It can be shown that the poles of $\tilde{G}_{kl}$ come from the zero's of D_{TM} and D_{TE} and therefore one must concentrate on D_{TM} and D_{TE} when considering possible poles which may be encountered when evaluating (1). When considering proper (non-leaky) modes on printed transmission lines, the integral in (1) can be performed along the real k_x axis. For improper (leaky) modes, however, to properly account for the exponential transverse growth of the leaky wave, the contour C must be deformed around appropriate poles of $\tilde{G}_{kl}$ in the complex k_x plane. The poles around which C is deformed correspond to the surface wave(s) or parallel mode(s) to which leakage occurs. The final contour C for a leaky wave can then be represented as the usual real axis integration plus the addition of a finite number of residues [2]. In the following section an efficient means of computing the real axis integration of (1) for multiconductor printed transmission lines is presented.

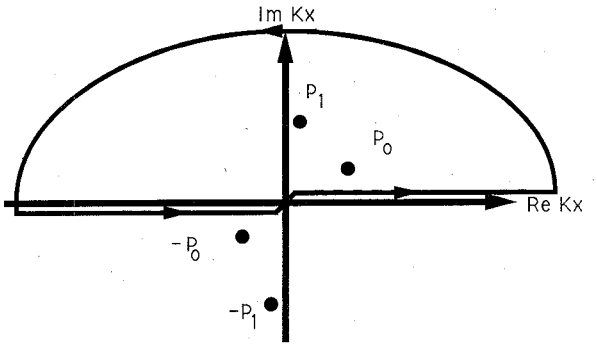

Fig. 2. Integration path for $\Delta > 0$. The semi-circle contribution to the integral vanishes, resulting in the real axis integration equaling an infinite summation of residues from poles in the top half of the k_x plane.

B. Asymptotic Technique

Consider the real axis integration of (1) for $\Delta > 0$. This integral is evaluated by enclosing the top half of the k_x plane, as shown in Fig. 2, and hence capturing all poles with Im $(k_x) > 0$. If $\Delta < 0$, the bottom half of the complex k_x plane is enclosed. The real axis contribution to (1) therefore becomes a summation of an infinite number of residues (each of which can be expressed in closed form):

$$I = 2\pi j \sum_{i=0}^{\infty} \mathrm{Res}\,(\sqrt{\Gamma_{ri}^2 - \gamma^2}) \qquad (3)$$

where Im $(\sqrt{\Gamma_{ri}^2 - \gamma^2}) > 0$. Implicit in (3), and as discussed above, all poles in (1) are from roots of $D_{\mathrm{TE}}(\Gamma^2)$ and $D_{\mathrm{TM}}(\Gamma^2)$. One also now sees the advantage (when appropriate, as in this study) of adding top and bottom shields to the numerical solution. By doing so, no branch cuts need be evaluated.

In general, an infinite number of terms are required in (3). For $\Delta/\lambda_o > 0.1$, however, it has been found that only a small number of terms are required (as will be shown below). The advantage of this approach is that as Δ/λ_o increases a real axis integration of (1) becomes increasingly inefficient due to the oscillatory nature of the integral while for such cases fewer and fewer residues are required to obtain convergence in (3).

To show the accuracy of this approach, consider the geometry in Fig. 1 with $\epsilon_r = 2.25$, $w1/s = w2/s = 0.4$, $sp/s = 0.6$, $d/s = 1.6$, $h2 = 0$, and $h1/s = 6.4$ where s is the separation between the centers of the two strips: $s = sp + w1$. The real axis contribution of (1) will be computed using Gauss–Legendre integration and with (3). In the example, a first order z-directed expansion function and a first order x-directed testing function are used in (1) and $k = x$, $l = z$, and $\Delta = s$. The basis functions used are trigonometric functions modified by the edge condition [1]. In Fig. 3(a) the real and imaginary parts of the integral are shown for the two integration techniques with $\beta/k_o = 1.3$ ($\alpha = 0$). For $s/\lambda_o < 0.155$ the agreement between the two methods is very good (and the integral is real). For $s/\lambda_o > 0.155$ the solution from (3) is complex while Gaussian integration gives a real solution that varies wildly. This suggests an inconsistency in the solution of the real axis contribution to (1) for $s/\lambda_o > 0.155$. This inconsistency involves the

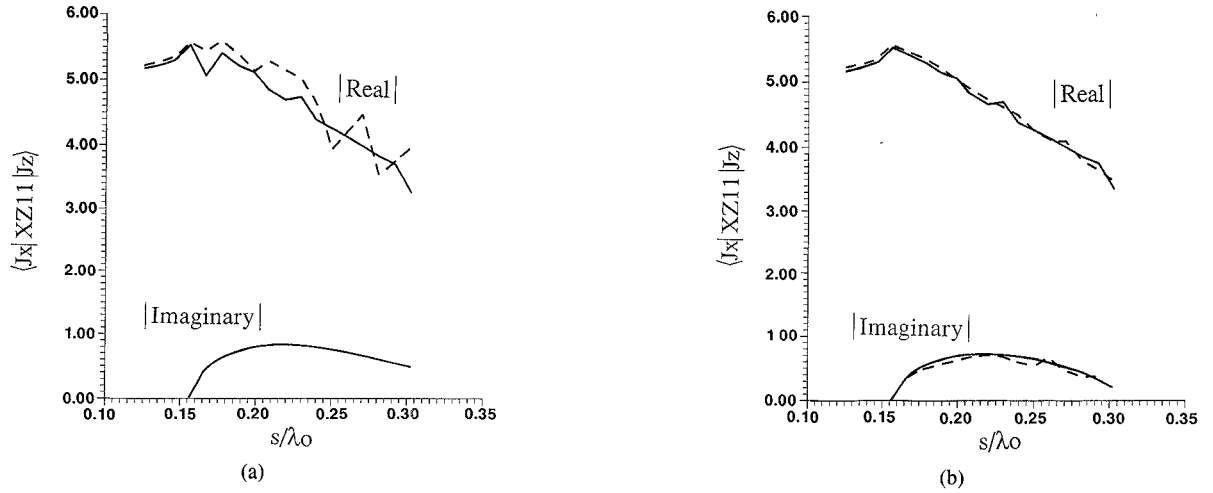

Fig. 3. Asymptotic (solid) and real axis integration (dashed) evaluation of $\langle J_x | G_{xz} | J_z \rangle$. Referring to Fig. 1, $\epsilon_r = 2.25$, $w1/sp = w2/sp = 0.66$, $d/sp = 2.66$, $h2 = 0$, and $h1/sp = 10.66$. The distance s is the separation between the two strip centers: $s = sp + w1$. In (a) $\gamma/k_o = 1.3$, in (b) $\gamma/k_o = 1.3$ for $S/\lambda_o < 0.155$ and $\gamma/k_o = 1.3 - j0.01$ for $s/\lambda_0 > 0.155$.

fact that for $s/\lambda_o > 0.155$, the first parallel plate mode has a phase constant that when normalized to k_o exceeds 1.3. Hence, to be consistent with the condition for the onset of leakage [2], γ must be complex for $s/\lambda_o > 0.155$ if $\beta/k_o < 1.3$. In Fig. 3(b) the same integral is computed except that for $s/\lambda_o > 0.155$ a complex $\gamma/k_o = 1.3 - j0.01$ is used in (3). The agreement between the two methods is now good for all s/λ_o. In the above calculations, 20 TE and 20 TM parallel plate modes were used in (3). This method provides a significant increase in computational efficiency and requires even fewer parallel plate modes when s/λ_o increases beyond the values in Fig. 3(a) and (b).

III. Results

A. Numerical Considerations

Finding γ (in general complex) requires the computation of matrix components of the form in (1). As alluded to above, trigonometric basis functions modified by the edge condition are used in this work. It was found that two even and two odd basis function for both the longitudinal and transverse current components on each strip was sufficient to yield convergence in all cases studied. The computation in (1) involves a real axis integration plus the addition of a finite number of closed form leaky wave poles when appropriate (for complex γ) [2]. When Δ in (1) satisfies $\Delta > 0.1\lambda_o$, the asymptotic procedure outlined above is used, significantly increasing the efficiency of the computations. In the results to be presented, 30 TE and 30 TM parallel plate modes were used in (3) for all $\Delta > 0.1\lambda_o$. The roots of the TE and TM parallel plate modes, Γ_n, need only be computed once for each frequency and all residues in (3) can be expressed in closed form. The use of 30 TE and TM modes was done to assure convergence for all $\Delta > 0.1\lambda_o$ encountered, but as Δ/λ_o increases, far fewer parallel plate modes need actually be considered. For the cases for which $\Delta < 0.1\lambda_o$, a standard real axis integration was applied. Typically, less than 5 min of CPU time was required for the computation of γ at each frequency on an IBM RISC 6000 workstation.

B. Example Calculations

To verify the accuracy of the numerical procedure outlined above, a comparison is made with results computed by Shigesawa *et al.* [7] using a mode matching technique for conductor-backed coplanar strips. In Fig. 4 are shown results for the real and imaginary parts of the propagation constant for the odd coplanar strip mode. One sees that for frequencies at which the phase constant of the odd coplanar strip mode is larger than that of the TM_0 parallel plate mode, the coplanar strip mode has a real propagation constant. At frequencies where this condition is not met, the coplanar strip mode is leaky and has a complex propagation constant. In Fig. 4 results are shown from a mode matching procedure [7] and from the method developed above. For the real part of the propagation constant, β, both methods predict a kink in the dispersion curve at the onset of leakage. There is a slight discrepancy between the β at frequencies at which leakage occurs. It should be noted, however, that Fig. 4(a) may be misleading since the two results never differ by more than 3% for all s/λ_o. For the imaginary part of the propagation constant, α, the two methods yield very similar results except for a slight shift in s/λ_o. The agreement between the two methods is reasonable considering the mode matching and spectral domain techniques are very different approaches with different convergence properties.

The second geometry is a coplanar strip transmission line, the results for which are shown in Fig. 5. The computations are compared with those in [2] (in which only β was given). The agreement between the computed results and those in [2] is good (over the entire frequency range, the results always differ by less than 1%).

IV. Conclusions

An efficient numerical procedure has been described for the analysis of dispersion and leaky waves on multilayered printed transmission lines. The problem was formulated in the spectral domain, which resulted in a matrix equation with components represented as spectral integrals. Making use of the fact that the fundamental zero-cutoff-frequency modes are slow waves, only leakage in the form of surface waves or parallel plate modes is possible. In the analysis, this allowed the placement of conducting shields above and below the transmission line system. This simplification, in addition to being appropriate for the problem under study, leads to a simple asymptotic expression in terms of a sum of closed form residues (no branch cut integrals). It was demonstrated that the

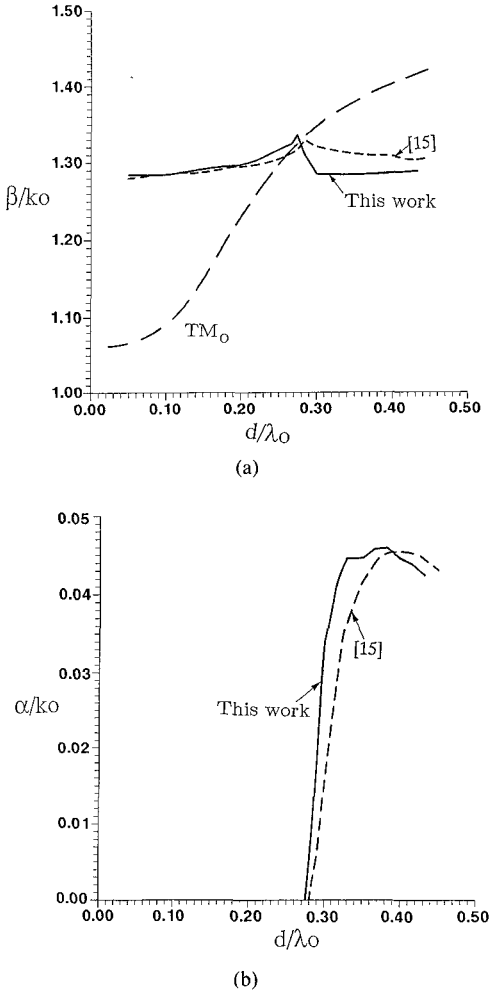

Fig. 4. Propagation constant γ for the odd conductor-backed coplanar strip mode. Referring to Fig. 1, $\epsilon_r = 2.25$, $w1/sp = w2/sp = 0.66$, $d/sp = 2.66$, $h2 = 0$, and $h1/sp = 10.66$; (a) gives β (and the propagation constant of the TM_0 parallel plate mode) and (b) gives α. A comparison is made between results computed using the method in this paper and with results computed previously using a mode matching analysis [7].

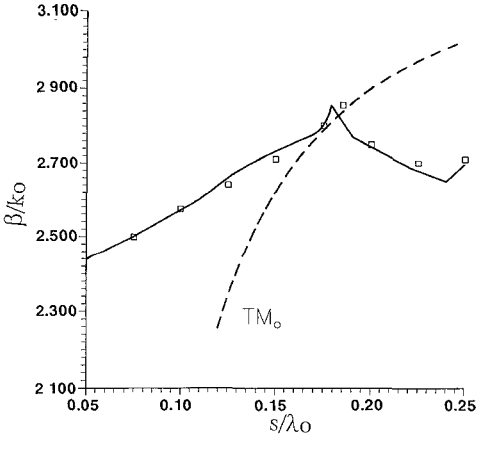

Fig. 5. Real part β of the propagation constant for coplanar strip transmission line. Referring to Fig. 1, $\epsilon_r = 10.5$, $w1/sp$ $w2/sp = 0.5$, $d/sp = 2.5$, and $h1/sp = h2/sp = 5$. The solid line represents the results of this work and the points represent the results of [2].

asymptotic procedure is accurate for expansion and testing functions separated by as few as 0.1 λ_o.

Acknowledgment

The author would like to express his gratitude to A. A. Oliner of Polytechnic University for several stimulating discussions on leaky waves and for providing the mode matching data in Fig. 4.

References

[1] L. Carin and K. J. Webb, "Isolation effects in single- and dual-plane VLSI interconnects," *IEEE Trans. Microwave Theory Tech.*, vol. 38, pp. 396-404, Apr. 1990.
[2] D. S. Phatak, N. K. Das, and A. P. Defonzo, "Dispersion characteristics of optically excited coplanar striplines: Comprehensive full wave analysis," *IEEE Trans. Microwave Theory Tech.*, vol 38, Nov. 1990.
[3] D. M. Pozar, "Input impedance and mutual coupling of rectangular microstrip antennas," *IEEE Trans. Antennas and Propagat.*, vol. AP-30, pp. 1191-1196, Nov. 1982.
[4] K. A. Michalski and D. Zheng, "Electromagnetic scattering and radiation by surfaces of arbitrary shape in a layered media, Part 1: Theory," *IEEE Trans. Antennas Propagat.*, vol. 38, pp. 335-344, Mar. 1990.
[5] M. Marin, S. Barkeshli, and P. H. Pathak, "Efficient analysis of planar microstrip geometries using a closed-form asymptotic representation of the grounded dielectric slab Green's function," *IEEE Trans. Microwave Theory Tech.*, vol. 37, pp. 669-679, Apr. 1989.
[6] K. A. Michalski, "On the efficient evaluation of integrals arising in the Sommerfeld halfspace problem," *Proc. IEEE*, vol. 132, pt. H, pp. 312-318, Aug. 1985.
[7] H. Shigesawa, M. Tsuji, and A. A. Oliner, private communication.

The Behavior of the Electromagnetic Field at Edges of Media with Finite Conductivity

Jochen Geisel, Karl-Heinz Muth, and Wolfgang Heinrich

***Abstract*—The principal behavior of both electric and magnetic fields at the edges of media with finite conductivity is investigated. We find that, as in the case of ideal conductors, the normal electric field shows a singularity at the edge. The magnetic field components, however, remain bounded if the permeabilities of the neighboring media do not differ. Detailed results on typical geometries are given.**

I. Introduction

It is well-known that singular points of the electric and the magnetic fields may occur at edges (e.g., [1], [2]). This is important, for instance, when checking the validity of surface integrals. Moreover, one can incorporate the order of singularity explicitly into numerical descriptions, which leads to very efficient modeling tools (e.g.: The basis functions used in the common spectral-domain approaches).

For the case of perfectly conducting media, detailed results are reported in the literature (see [1], [2]). Fig. 1 shows the corresponding geometry and the notation used here. A cylindrical coordinate system is used. We consider the equivalent 2-dimensional

Manuscript received January 24, 1991; revised July 22, 1991.
The authors are with the Institut fur Hochfrequenztechnik, Technische Hochschule Darmstadt, Merckstrasse 25, W-6100 Darmstadt, Germany.
IEEE Log Number 9103900.